



HAL
open science

Large global variations in measured airborne metal concentrations driven by anthropogenic sources

Jacob Mcneill, Graydon Snider, Crystal L. Weagle, Brenna Walsh, Paul Bissonnette, Emily Stone, Ihab Abboud, Clement Akoshile, Nguyen Xuan Anh, Rajasekhar Balasubramanian, et al.

► **To cite this version:**

Jacob Mcneill, Graydon Snider, Crystal L. Weagle, Brenna Walsh, Paul Bissonnette, et al.. Large global variations in measured airborne metal concentrations driven by anthropogenic sources. *Scientific Reports*, 2020, 10, 10.1038/s41598-020-78789-y . insu-03671641

HAL Id: insu-03671641

<https://insu.hal.science/insu-03671641>

Submitted on 19 May 2022

HAL is a multi-disciplinary open access archive for the deposit and dissemination of scientific research documents, whether they are published or not. The documents may come from teaching and research institutions in France or abroad, or from public or private research centers.

L'archive ouverte pluridisciplinaire **HAL**, est destinée au dépôt et à la diffusion de documents scientifiques de niveau recherche, publiés ou non, émanant des établissements d'enseignement et de recherche français ou étrangers, des laboratoires publics ou privés.



Distributed under a Creative Commons Attribution 4.0 International License



OPEN

Large global variations in measured airborne metal concentrations driven by anthropogenic sources

Jacob McNeill^{1,2}, Graydon Snider³, Crystal L. Weagle^{2,3}, Brenna Walsh^{2,3}, Paul Bissonnette³, Emily Stone³, Ihab Abboud⁴, Clement Akoshile⁵, Nguyen Xuan Anh⁶, Rajasekhar Balasubramanian⁷, Jeffrey R. Brook⁸, Craig Coburn⁹, Aaron Cohen¹⁰, Jinlu Dong¹¹, Graham Gagnon¹², Rebecca M. Garland^{13,14,15}, Kebin He¹⁶, Brent N. Holben¹⁷, Ralph Kahn¹⁷, Jong Sung Kim¹⁸, Nofel Lagrosas¹⁹, Puji Lestari²⁰, Yang Liu²¹, Farah Jeba²², Khaled Shaifullah Joy²², J. Vanderlei Martins²³, Amit Misra²⁴, Leslie K. Norford²⁵, Eduardo J. Quel²⁶, Abdus Salam²², Bret Schichtel²⁷, S. N. Tripathi²⁴, Chien Wang²⁸, Qiang Zhang¹⁶, Michael Brauer²⁹, Mark D. Gibson^{12,30}, Yinon Rudich³¹ & Randall V. Martin^{1,2,3}✉

Globally consistent measurements of airborne metal concentrations in fine particulate matter (PM_{2.5}) are important for understanding potential health impacts, prioritizing air pollution mitigation strategies, and enabling global chemical transport model development. PM_{2.5} filter samples (N ~ 800 from 19 locations) collected from a globally distributed surface particulate matter sampling network (SPARTAN) between January 2013 and April 2019 were analyzed for particulate mass and trace metals content. Metal concentrations exhibited pronounced spatial variation, primarily driven by anthropogenic activities. PM_{2.5} levels of lead, arsenic, chromium, and zinc were significantly enriched at some locations by factors of 100–3000 compared to crustal concentrations. Levels of metals in PM_{2.5} and PM₁₀ exceeded health guidelines at multiple sites. For example, Dhaka and Kanpur sites

¹Department of Chemistry, Dalhousie University, Halifax, Canada. ²Department of Energy, Environmental and Chemical Engineering, Washington University in St. Louis, St. Louis, MO, USA. ³Department of Physics and Atmospheric Science, Dalhousie University, Halifax, Canada. ⁴Environment and Climate Change Canada, Downsview, ON, Canada. ⁵Department of Physics, University of Ilorin, Ilorin, Nigeria. ⁶Institute of Geophysics, Vietnam Academy of Science and Technology, Hanoi, Vietnam. ⁷Department of Civil and Environmental Engineering, National University of Singapore, Singapore, Singapore. ⁸Department of Public Health Sciences, University of Toronto, Toronto, ON M5S 1A8, Canada. ⁹Department of Geography and Environment, University of Lethbridge, Lethbridge, AB, Canada. ¹⁰Health Effects Institute, 75 Federal Street Suite 1400, Boston, MA 02110-1817, USA. ¹¹School of Environment, Tsinghua University, Beijing, China. ¹²Department of Civil and Resource Engineering, Dalhousie University, Halifax, Canada. ¹³Council for Scientific and Industrial Research (CSIR), Pretoria, South Africa. ¹⁴Unit for Environmental Sciences and Management, North-West University, Potchefstroom, South Africa. ¹⁵Department of Geography, Geo-Informatics and Meteorology, University of Pretoria, Pretoria, South Africa. ¹⁶Department of Earth System Science, Tsinghua University, Beijing, China. ¹⁷Earth Science Division, NASA Goddard Space Flight Center, Greenbelt, MD, USA. ¹⁸Department of Community Health and Epidemiology, Dalhousie University, Halifax, Canada. ¹⁹Manila Observatory, Ateneo de Manila University Campus, Quezon City, Philippines. ²⁰Faculty of Civil and Environmental Engineering, Bandung Institute of Technology (ITB), JL. Ganesha No.10, Bandung 40132, Indonesia. ²¹Gangarosa Department of Environmental Health, Rollins School of Public Health, Emory University, Atlanta, GA 30322, USA. ²²Department of Chemistry, Faculty of Science, University of Dhaka, Dhaka 1000, Bangladesh. ²³Department of Physics and Joint Center for Earth Systems Technology, University of Maryland, Baltimore County, Baltimore, MD, USA. ²⁴Center for Environmental Science and Engineering, Department of Civil Engineering, Indian Institute of Technology Kanpur, Kanpur, India. ²⁵Department of Architecture, Massachusetts Institute of Technology, Cambridge, MA 02139, USA. ²⁶UNIDEF (CITEDEF-CONICET), Juan B. de la Salle 4397 – B1603ALO Villa Martelli, Buenos Aires, Argentina. ²⁷Cooperative Institute for Research in the Atmosphere, Colorado State University, Fort Collins, CO, USA. ²⁸Laboratoire d'Aerologie, CNRS/UPS, 14 Avenue Edouard Belin, Toulouse, France. ²⁹School of Population and Public Health, University of British Columbia, Vancouver, BC, Canada. ³⁰AirPhoton, LLC., Baltimore, MD, USA. ³¹Department of Earth and Planetary Sciences, Weizmann Institute, 76100 Rehovot, Israel. ✉email: rvmartin@wustl.edu

exceeded the US National Ambient Air 3-month Quality Standard for lead (150 ng m^{-3}). Kanpur, Hanoi, Beijing and Dhaka sites had annual mean arsenic concentrations that approached or exceeded the World Health Organization's risk level for arsenic (6.6 ng m^{-3}). The high concentrations of several potentially harmful metals in densely populated cities worldwide motivates expanded measurements and analyses.

Many regions of the world far exceed the World Health Organization (WHO) air quality guidelines for ambient fine particulate matter ($\text{PM}_{2.5}$)^{1,2} air pollution levels, with substantial impacts on human health³. The Global Burden of Disease estimated 3 million deaths (9% of all deaths) and 80 million years of lost healthy life were attributable to exposure to outdoor $\text{PM}_{2.5}$ globally in 2017⁴. Nonetheless, ground-based monitoring of $\text{PM}_{2.5}$ mass concentration is inadequate for exposure assessment⁵, and the select studies of $\text{PM}_{2.5}$ chemical composition measurements^{6,7} are even sparser. In some locations, the majority of metal concentration measurements made to date have been of the PM_{10} fraction^{8–10}. Global observations of $\text{PM}_{2.5}$ mass concentration and composition can inform aerosol model development and exposure assessment, improve understanding of emission sources and help prioritize mitigation policies¹¹ to reduce health impacts.

The relationship between $\text{PM}_{2.5}$ and human health^{12,13} including the association of $\text{PM}_{2.5}$ with cardiovascular disease¹⁴, respiratory disease¹⁵, cancer¹⁶, and type 2 diabetes¹⁷ has become better understood over the last few decades. However, more analysis of these relationships is needed before effects of particular components (specifically trace metals) are well understood at a global scale. The oxidative potential of $\text{PM}_{2.5}$ is related to its metal content⁶ (as well as its carbon content¹⁸) and increased abundance of redox-active elements can induce oxidative stress^{19–22}. Increased cardiovascular disease rates have been associated with exposure to enhanced relative concentrations of K, Al, Ni, Zn and V^{14,23} and mortality risks have been associated with preferential bioaccumulation of heavy metals such as As, Pb, and Al²⁴. Further, many metals have known health effects, such as As, Cd, and Cr, which are classified by the WHO's International Agency for Research on Cancer (IARC) as known human carcinogens (IARC Group 1)²⁵, and Pb, which is associated with impaired cognitive function²⁶. Measurements of $\text{PM}_{2.5}$ composition are needed to assess the global distribution of these deleterious metals in fine particulate matter, as they could pose health risks to populations living in areas of high $\text{PM}_{2.5}$ pollution.

Ground-based elemental composition can also provide information about airborne $\text{PM}_{2.5}$ sources. For example, K has associations with wood burning^{27–29}, Zn can be linked with traffic through tire wear³⁰, and V derives mainly from heavy fuel oil combustion such as from shipping^{31,32}. Coal is a source of multiple potentially harmful elements such as Pb, Cr, Mn, As, and Se^{31,33} whereas non-ferrous metal production is a large source of As, Cd, and Zn³¹. Vehicle traffic contributes a mix of elements including the heavy metals Ba, Zn, and Pb, as well as the crustal components Fe, Al, Mg, and Ti^{27,34}. To our knowledge, no other global network has measured the trace metal concentrations in $\text{PM}_{2.5}$. These observations are needed to better understand particulate matter sources and loadings, to assess emerging emission inventories and evaluate spatially-resolved concentration predictions made by chemical transport models on a global scale^{35,36} and to understand local and regional impacts of emission sources.

The ground-based Surface PARTiculate mAtter Network (SPARTAN; <http://www.spartan-network.org>) is building up a long-term data set measuring PM concentration at globally distributed sites³⁷ and provides new data to evaluate PM composition. In this study, we investigate the trace metal composition of $\text{PM}_{2.5}$, supplemented by coarse PM ($\text{PM}_c = \text{PM}_{10-2.5}$) and PM_{10} data, in ambient air samples from SPARTAN sites around the world. Our focus is on $\text{PM}_{2.5}$ due to its importance for health.

Results and discussion

The mean $\text{PM}_{2.5}$ mass concentrations at each SPARTAN site are shown in Fig. 1, with standard error bars ($\text{SE} = \sigma / \sqrt{n}$, σ = sample standard deviation, n = number of samples) for each site mean. Of the 19 SPARTAN sites, Kanpur had the highest mean $\text{PM}_{2.5}$ levels at 102.8 ± 20.2 (SE) $\mu\text{g}/\text{m}^3$, followed by Beijing at 58.1 ± 2.2 $\mu\text{g}/\text{m}^3$, then Dhaka (49.0 ± 3.3 $\mu\text{g}/\text{m}^3$) and Hanoi (47.1 ± 7.6 $\mu\text{g}/\text{m}^3$).

Sites located in urban areas situated outside of North America generally had the highest levels of $\text{PM}_{2.5}$. The one notable exception was the Mammoth Cave site, which had the 11th highest $\text{PM}_{2.5}$ levels. This can be explained through two aspects of the sampling; firstly, the site is located in a heavily wooded national park; sampling occurred in the summer when carbonaceous emissions are highest from biogenic sources, and secondary organic aerosol is prevalent³⁸. Secondly, the site has the second-lowest percentage of its $\text{PM}_{2.5}$ mass present in the measured trace metal mass (4%), indicating other sources (i.e. biogenic) were dominant. Sites located in Canada generally had the lowest levels of $\text{PM}_{2.5}$, which is consistent with their intended categorization as low-PM environments.

Table 1 details the mean mass concentrations of 15 trace metals analyzed in $\text{PM}_{2.5}$ samples from SPARTAN sites. Elements above ICP-MS detection limits (detailed in supplemental Table S1) for > 10% of samples were considered; Li, Co, Ag, and Ce did not satisfy this requirement, and as such are not discussed here. Individual elements were examined to understand their distributions across sites (a detailed breakdown across sites can be found in the supplemental section S1, with a corresponding table of standard deviations in supplemental Table S4). Elemental breakdowns for the PM_{10} fraction are found in supplemental Table S7, while relative concentrations of each trace element in $\text{PM}_{2.5}$ can be found in supplemental Table S8.

Whole-system uncertainties for the SPARTAN network were calculated in the same manner as previously reported by Weagle and coauthors³⁹. The results for the uncertainties can be found in the supplemental Table S3, and individual plots in supplemental Figure S1.

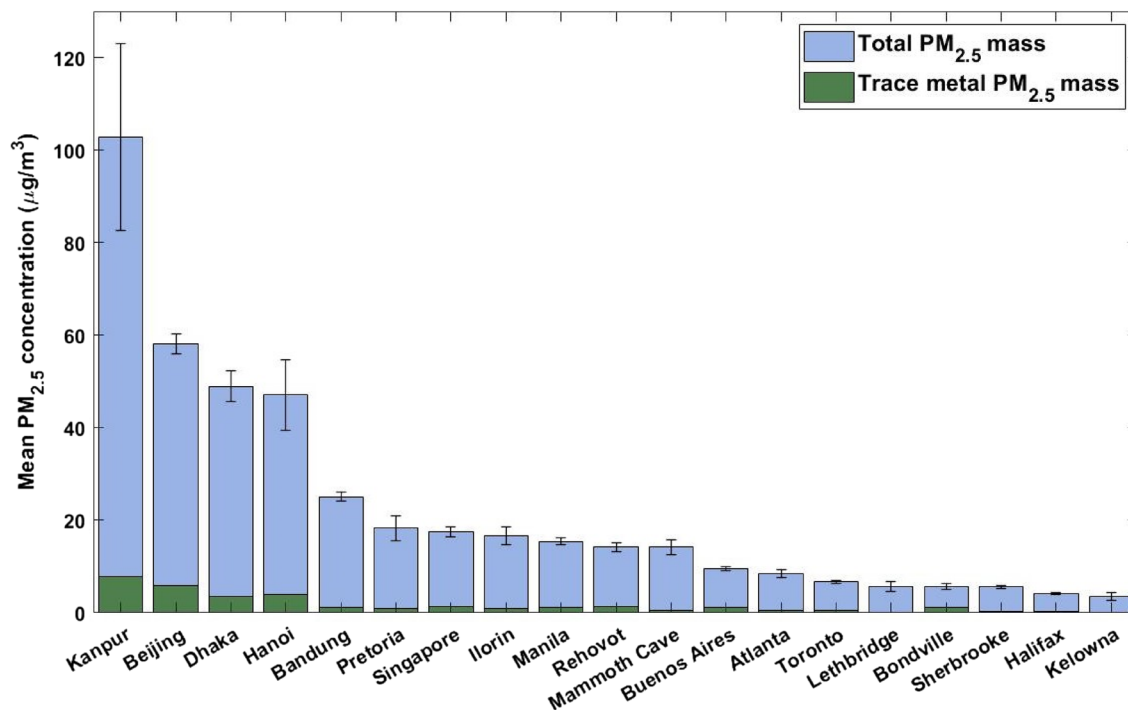


Figure 1. Mean $PM_{2.5}$ mass concentrations at SPARTAN sites with standard error bars shown. Overlaid green bars show total measured trace metal mean mass concentrations for each site.

	$PM_{2.5}$	K	Mg	P	Ti	V	Cr	Mn	Fe	Cu	Zn	As	Se	Cd	Ba	Pb
Mammoth Cave	14.2	74.8	28.0	55.7	1.01	0.78	1.20	1.84	83.2	3.68	8.5	0.26	0.28	0.05	3.12	0.90
Atlanta	8.6	27.8	11.5	105.3	1.24	0.18	4.20	0.71	51.5	3.67	9.3	0.56	0.54	0.02	5.41	1.08
Bandung	25.1	432.1	18.3	23.9	1.73	0.31	2.12	2.80	78.2	3.28	23.7	0.60	0.23	0.32	2.57	34.62
Beijing	58.1	962.6	177.3	151.1	11.18	2.30	4.39	23.84	394.7	26.73	101.5	7.12	67.40	3.29	21.81	41.30
Bondville	5.7	64.1	34.1	162.3	1.39	0.13	3.77	1.59	37.0	3.11	16.7	0.65	0.55	0.12	2.15	1.54
Buenos Aires	9.6	152.1	30.4	30.3	1.70	2.48	1.10	2.52	94.0	5.17	20.8	0.43	0.36	0.30	5.08	10.47
Dhaka	49.0	876.0	47.9	23.0	3.94	6.98	8.00	25.40	167.7	11.69	498.4	6.33	5.38	7.35	12.53	279.72
Halifax	4.2	40.0	17.8	1.1	0.25	0.23	0.39	0.36	10.8	0.76	3.7	0.14	0.07	0.00	0.75	0.49
Hanoi	47.1	1293.8	84.5	36.6	5.21	2.10	2.28	80.05	282.2	14.10	1178.8	8.11	3.00	4.25	7.13	141.04
Ilorin	16.6	355.6	15.5	5.1	0.88	0.61	47.96	4.51	182.4	0.94	12.9	0.22	0.14	0.06	0.90	4.27
Kanpur	102.8	3047.1	74.4	340.1	5.60	2.21	19.41	9.89	168.0	8.78	119.5	15.29	10.60	12.88	3.99	209.33
Kelowna	3.5	34.1	2.4	1.6	0.32	0.14	0.32	0.41	17.0	0.55	1.4	0.19	0.04	0.01	0.75	0.29
Lethbridge	6.2	56.3	6.4	1.5	0.30	0.03	0.25	0.68	18.5	0.76	1.9	0.17	0.14	0.03	0.85	0.38
Manila	15.4	253.3	20.3	34.4	1.30	2.32	2.97	3.17	111.2	2.93	29.4	0.33	0.96	0.25	2.31	5.89
Pretoria	18.3	220.0	14.8	37.5	1.66	0.44	0.80	5.78	105.2	2.28	27.5	1.00	0.54	0.10	2.54	4.88
Sherbrooke	5.7	48.3	5.0	4.3	0.45	0.03	0.20	0.92	16.7	0.73	4.2	0.26	0.10	0.02	0.58	1.08
Rehovot	15.4	135.2	79.9	11.4	2.18	2.95	1.56	2.82	123.5	3.22	12.8	0.26	0.34	0.09	3.69	4.64
Singapore	17.5	344.9	24.2	13.4	1.66	37.92	0.47	7.76	89.9	5.57	110.1	0.48	0.71	0.12	3.80	3.54
Toronto	6.7	71.0	12.0	9.7	0.83	0.09	0.72	1.59	46.5	2.71	10.7	0.31	0.29	0.04	3.82	1.38

Table 1. Full elemental breakdown of mean mass concentrations of trace metals in $PM_{2.5}$ at SPARTAN sites. Mass concentrations of each trace metal are reported in ng/m^3 . Total $PM_{2.5}$ mass concentrations are reported in $\mu g/m^3$. Corresponding standard deviations can be found in the supplemental Table S4.

Of interest is the anthropogenic contribution to such trace metals in general. Crustal enrichment factors (EFs) were used to distinguish naturally occurring crustal elements from those released by anthropogenic sources. We compared filter-extracted elemental concentrations X to background continental concentrations from Taylor and McLennan⁴⁰, normalized by measured crustal Fe concentrations, which is predominantly from natural sources (e.g.⁴¹) as seen in Eq. (1).

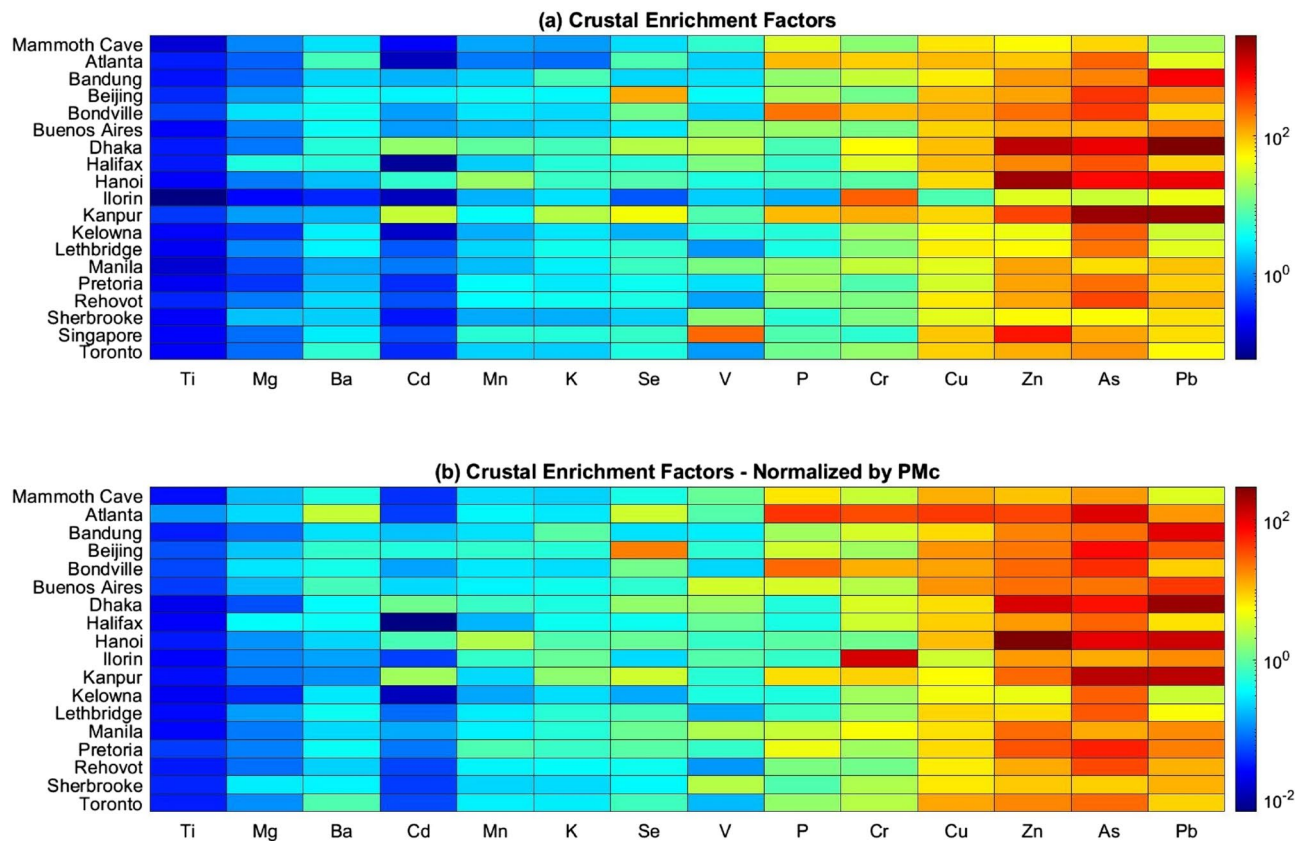


Figure 2. (a) Crustal enrichment factors (EF) for $PM_{2.5}$ relative to crustal ratios of the given element and iron (Eq. 1), and (b) replacing measured iron with measured PM_c (Eq. 2). Elements are sorted by mean enrichment factor across all sites; sites are listed alphabetically. Singapore is not shown in the bottom plot due to unavailable PM_c data.

$$EF_{X,2.5} = \frac{\left[\frac{X}{Fe} \right]_{PM_{2.5}}}{\left[\frac{X}{Fe} \right]_{Taylor}} \quad (1)$$

Although natural variability in the Fe fraction in soil will affect these results, the Fe fraction in soil tends to be quite consistent⁴². Anthropogenic sources of Fe imply that the resultant enhancement ratios will be a conservative indicator of anthropogenic contribution. Nonetheless, to ensure that conclusions are not affected by using Fe as the reference element due to extraction efficiency, a complementary analysis was performed by replacing site Fe concentrations with corresponding coarse PM concentrations, seen in Eq. (2). Coarse particulate matter over land has been established as predominantly stemming from suspended dust^{43,44} (with other potential sources including urban dust and organic material), making it a suitable measure of crustal source abundance to verify the validity of results using Fe. An estimate of the concentrations of the metal oxides present in coarse PM (estimated coarse PM = PM_c^*) was obtained by use of the soil reconstruction equation described by Malm et al.⁴³ and shown in Eq. (3), in combination with continental concentrations from Taylor and McLennan.

$$EF_{X,2.5} = \frac{\left[\frac{X}{PM_c} \right]_{PM_{2.5}}}{\left[\frac{X}{PM_c^*} \right]_{Taylor}} \quad (2)$$

$$PM_c^* = 2.20[Al] + 2.49[Si] + 1.63[Ca] + 2.42[Fe] + 1.94[Ti] \quad (3)$$

Enrichment factors can be considered in three subsets: $EF < 10$, elements which we attribute to sources that are primarily crustal^{45–47}; EF between 10 and 100, elements with mixed anthropogenic and natural sources; and $EF > 100$, elements with largely anthropogenic sources. Figure 2 displays the EF elemental breakdown for all SPARTAN sites as well as the site-specific PM_c -scaled EF results.

Similar results when normalizing by either Fe or PM_c provides confidence in the analysis. Enrichment factors vary by orders of magnitude depending on element and location. The highest levels of enrichment are found in anthropogenically-dominant elements such as Pb, As, and Zn, and generally found at sites with the highest

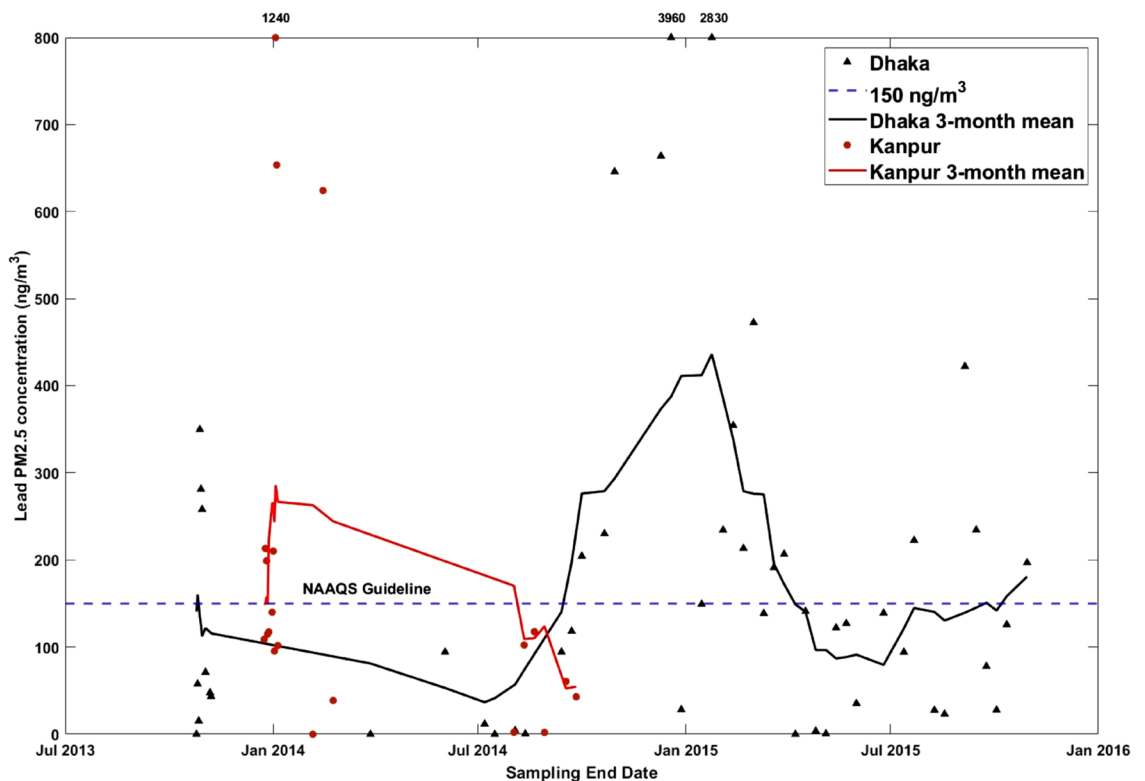


Figure 3. Concentrations of Pb in SPARTAN samples at Kanpur (red circles) and Dhaka (black triangles). Dotted blue line represents the NAAQS 3-month exposure guideline for lead concentrations (150 ng/m^3). Samples are plotted by the final date of sampling, as sampling occurs over a time period of 9 days. Solid red (Kanpur) and black (Dhaka) lines represent 3-month rolling mean Pb concentrations.

levels of $\text{PM}_{2.5}$. Of the four sites with the greatest $\text{PM}_{2.5}$ concentrations, elemental EF values > 350 are found in Dhaka, Kanpur, and Hanoi for Pb, Zn, and As, and in Beijing for As. These enrichments highlight the effects of anthropogenic activities not only on total $\text{PM}_{2.5}$ but on trace metal $\text{PM}_{2.5}$ specifically, with potentially harmful levels of these heavy metals found in these high-PM cities.

Of the individual elements measured, two elements in particular demand further investigation: the carcinogenic metalloid As, and the heavy metal Pb. These elements can originate from multiple industrial sources, including smelting, waste incineration, and coal burning^{12,14}. There are guidelines for the concentrations in air of both elements. For example, the US National Ambient Air Quality (NAAQS) exposure limit for Pb is a 3-month mean concentration of 150 ng/m^3 ³⁴⁸, and multiple samples taken from the Kanpur and Dhaka sites exceeded these Pb concentrations—leading to 3-month mean concentrations over the US guideline for both sites. Figure 3 shows the lead $\text{PM}_{2.5}$ concentrations measured in samples taken from the two sites, with the NAAQS guideline as a reference. This guideline refers to Total Suspended Particulate matter (TSP), a wider size range of particulates, so measured concentrations of lead $\text{PM}_{2.5}$ are underestimating the TSP concentrations.

A comparison of the $\text{PM}_{2.5}$ (Table 1) and PM_{10} (Table S7) values reveals that site-mean PM_{10} values are 41% higher at Kanpur and 74% higher at Dhaka than the $\text{PM}_{2.5}$ values. Comparing $\text{PM}_{2.5}$ at the two sites, Dhaka has both a higher mean Pb concentration (280 ng/m^3) than Kanpur (209 ng/m^3), and more samples measuring above the 150 ng/m^3 guideline (38% vs. 30%). This is in contrast to their respective levels of total $\text{PM}_{2.5}$, as mean $\text{PM}_{2.5}$ concentrations from Kanpur samples are roughly double those in Dhaka. The Dhaka site exhibits some seasonality, with peak Pb values occurring around January 2015 and generally high values in winter months, when mixed layer depths are shallow. Similarly high Pb levels in $\text{PM}_{2.5}$ have previously been reported in Dhaka^{49,50}, and have been attributed to combustion of fossil fuels, battery industries, paints and varnishes, and lead-containing waste water.

The second element of interest in this study is arsenic, as the World Health Organization recommends no safe level of arsenic exposure due to its carcinogenic risk. An estimated lifetime excess risk is 1:1,000,000 at 0.66 ng/m^3 , or 1:100,000 at 6.6 ng/m^3 ³⁵¹. As is associated with industrial activities such as smelting, burning of coal, and waste incineration^{52–54}. Mean As concentrations for SPARTAN sites are shown in Fig. 4. The majority of SPARTAN sites fall under this level, but there are four sites with mean As concentrations near or above 6.6 ng/m^3 —Kanpur, Hanoi, Beijing, and Dhaka. The Beijing and Dhaka sites were sampled for an entire year facilitating direct comparison with the guideline. Although sampling at Kanpur and Hanoi was less than a year, concentrations at these sites were sufficiently high that the standard would be approached or exceeded even in the unlikely event that ambient concentrations were zero for the remainder of the year (yielding roughly 11.5 ng/m^3 for Kanpur and 6.1 ng/m^3 for Hanoi).

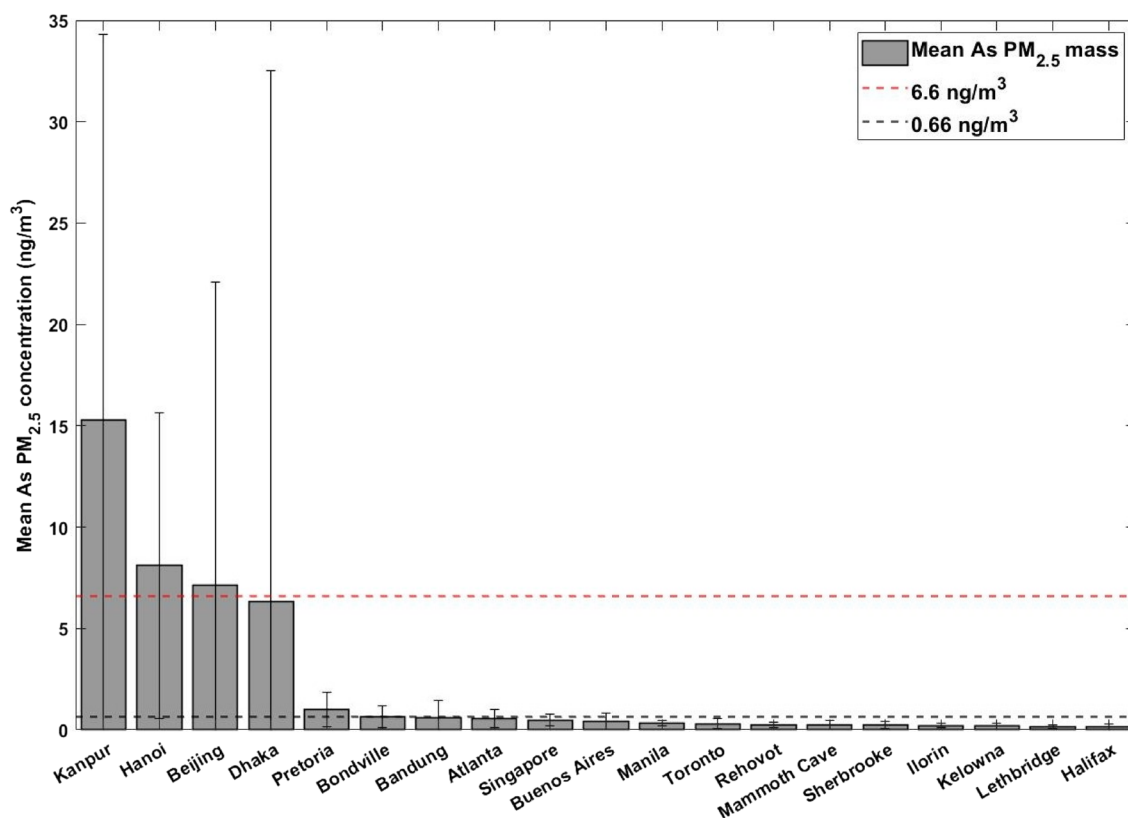


Figure 4. Concentrations of As in PM_{2.5} samples taken from SPARTAN sites, with standard deviation bars shown. Dotted red line represents 1:100,000 excess lifetime risk of cancer due to As exposure (6.6 ng/m³). Dotted black line represents 1:1,000,000 excess lifetime risk of cancer due to arsenic exposure (0.66 ng/m³).

Kanpur has significantly higher As concentrations than any other SPARTAN site with 15.3 ng/m³. The mean As mass concentrations for Hanoi, Beijing, and Dhaka were determined to be 8.1 ng/m³, 7.1 ng/m³, and 6.3 ng/m³ respectively. These sites are also the four sites with the highest levels of PM_{2.5}, so it is not unexpected that they have greater abundances of trace metal PM_{2.5} such as arsenic.

A complementary approach to understanding the levels of trace metals in fine PM at SPARTAN sites is to compare them not only to the crustal abundance, but to another site with relatively low levels of these trace metals. Figure 5 shows the relative abundance (RA) of PM_{2.5} trace metals at the eight SPARTAN sites with at least one elemental RA of 10 or greater, compared to a natural reference site, in this case the Mammoth Cave (M.C.) National Park site. The Mammoth Cave site has the second-lowest trace metal mass percentage of total PM_{2.5} mass. Low trace metals and the natural environment of the site make it an insightful reference point against which to compare the various types of SPARTAN sites. Relative abundances for trace metal PM_{2.5} are calculated using Eq. (4) and are unitless.

$$RA_X = [X]_{\text{Site}}/[X]_{\text{M.C.}} \quad (4)$$

Sites with an elemental RA of 10 or greater are shown in the figure below to highlight particular areas and species of note. The full set of relative abundances can be found in the supplemental information (Table S5), as well as a similar calculation using the PM_{2.5}-relative elemental concentrations instead of the absolute concentrations (supplemental Table S6). Generally, combustion-related elemental concentrations increase together, as do crustal components.

Particularly high RA values (12–311) of anthropogenic elements Zn, As, Pb, and Cd are found for Kanpur, Beijing, Dhaka, and Hanoi; these abundances are in alignment with the crustal enrichments seen for these heavy metals at these sites, and with the higher PM_{2.5} levels at these sites.

Examining the relative abundances on a site-specific basis reveals more local information—one notable instance being the Beijing site, which shows markedly elevated levels of selenium compared to any other site. Chinese coal has been found to be particularly rich in selenium⁵⁵, which in concert with the large quantity of coal burned in China implies coal-burning as a major anthropogenic source of selenium PM_{2.5} in the region. Coal emissions in China have also been shown to contain high levels of As, Cd, and Pb⁵⁶, all of which are significantly elevated by RA in the PM_{2.5} samples from Beijing.

There are a few isolated, notable RA values at the Bandung and Ilorin sites that can be linked to specific regional industries. Bandung has highly elevated Pb (RA of 38, EF > 700), even after the phasing out of leaded gasoline in 2006⁵⁷. One likely contributor to the extremely high Pb levels is lead smelting, as Indonesia is one of the largest lead acid battery recyclers in Asia⁵⁸. Rapidly growing numbers of lead smelters produce large amounts

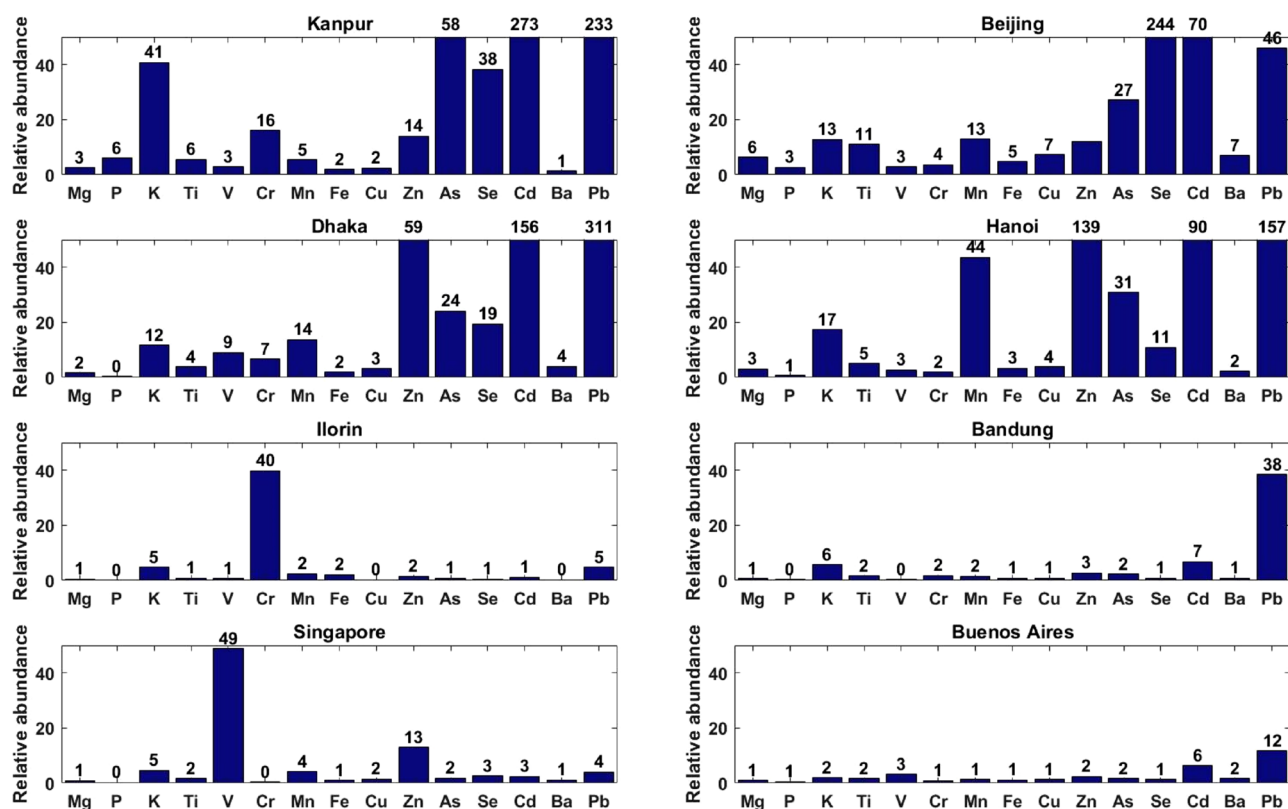


Figure 5. Relative abundances of trace metals in $PM_{2.5}$ in representative SPARTAN sites with at least one element with RA of 10 or greater. Abundances are relative to the natural, low-trace metal $PM_{2.5}$ Mammoth Cave site. Sites are sorted by total $PM_{2.5}$ mass concentrations L-R, then top to bottom. Relative abundance values are unitless.

of Pb-enhanced emissions, the transport of which could explain the elevated lead levels seen at the Bandung site. The Ilorin site shows abundant levels of Cr (RA of 40, EF > 260); this may be associated with the prevalent tanning industry in the region, in which chromium compounds are used prominently. Analysis of effluents from Nigerian tanneries found high levels of Cr present⁵⁹, and high levels of the metal in $PM_{2.5}$ imply that some of this Cr is being converted to or released in particulate form.

Singapore has significant enrichment of V (49), which likely stems from the nearby burning of shipping fuel, with the Port of Singapore being one of the busiest ports in the world. Proximity to petroleum refineries is another likely contributor to these elevated V levels⁶⁰, as the Singapore site is located approximately 10 km east-northeast of Jurong Island, an industrialized artificial island home to several refineries⁶¹. Significantly enhanced levels of V in Singapore can also be seen in the crustal EFs (EF > 240, the highest for V of any SPARTAN site), which further validates the key impact of nearby anthropogenic emissions. The influence of these and other nearby anthropogenic activities (e.g. vehicular traffic and metal production facilities) is also seen in enhanced levels of Zn, with an RA value of 13 and EF > 600. Unlike some of the other regions with high $PM_{2.5}$ and significant anthropogenic activity, Singapore does not exhibit large relative abundances for other anthropogenically dominant elements such as Pb, As, and Cr. This is likely due to the near-total absence of coal-burning in the region, as Singapore relies heavily on natural gas for energy purposes⁶¹.

Two non-North American sites did not exhibit any RA values of 10 or higher: Manila and Rehovot. This merits attention as Manila in particular is a densely populated city yet shows no significantly higher levels of trace metals than our natural site in Mammoth Cave. One partial explanation is that Manila has relatively low $PM_{2.5}$ mass concentrations among the non-North American sites (8th out of 11 sites). For Rehovot, the sampling site is the least densely populated non-North American site, which would align with the generally low amounts of trace metals observed at that location. Of the North American sites, Toronto, Bondville, Sherbrooke, Atlanta, Halifax, Kelowna, and Lethbridge all had RA values below 5 for all elements measured. This aligns well with expectations that these sites should generally have less PM pollution, especially for the Canadian MAPLE (Mortality Air Pollution Associations in Low Exposure Environments) sites designated as low-PM environments.

Although SPARTAN does not yet have sites in Europe, we surveyed prior measurements from the region to place our findings elsewhere in context. We find that at European background reference sites, heavy metal concentrations tended to be lower than at SPARTAN sites in densely populated regions^{62,63}. These findings reinforce our conclusions about the enrichment of heavy metals compared with background reference sites.

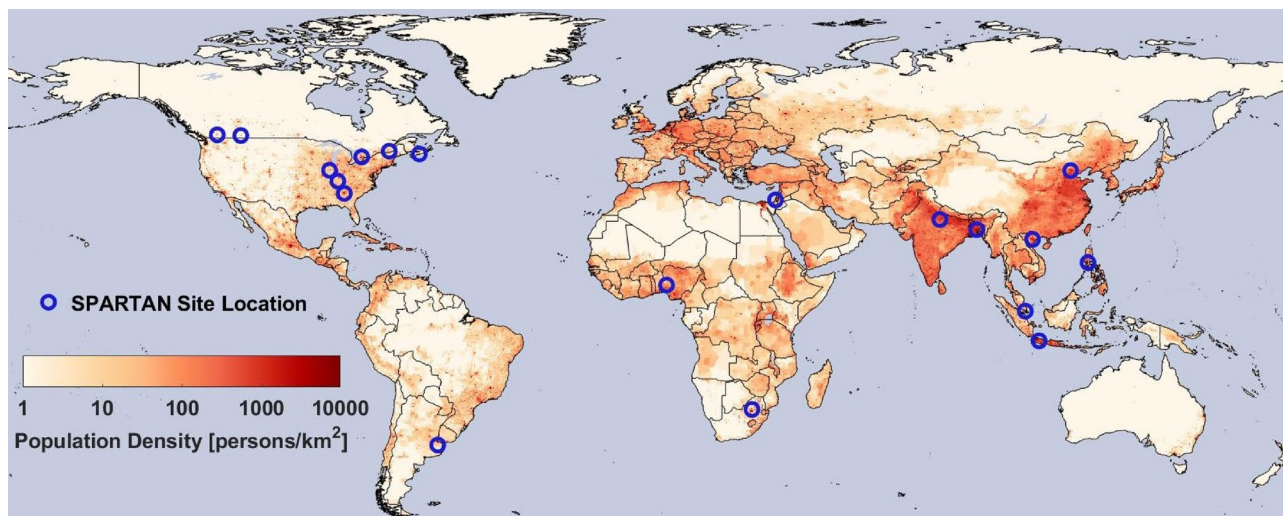


Figure 6. Open blue circles indicate the location of SPARTAN sampling sites used here, overlaid on a background color map of population density (NASA SEDAC GPW⁶⁵, made using MATLAB R2019b—<https://www.mathworks.com/products/matlab.html>).

Conclusions and implications

Globally consistent measurements of airborne metal concentrations in $PM_{2.5}$ are needed to assess and understand the distributions of ambient concentrations. Over 800 samples of fine particulate matter ($PM_{2.5}$) from 19 unique sampling sites located across four continents were collected and analyzed using consistent protocols, with concentrations of 15 different trace metals reported. As the SPARTAN network continues to develop, these sampling protocols will continue to be improved to better report the chemical composition of trace metals in $PM_{2.5}$. In general, it was found that several elements were enriched compared to their concentrations in the crust—in particular, elements such as Pb, As, and Zn that have anthropogenic sources were greatly enriched in sampled $PM_{2.5}$. This enrichment was most notable in large, densely populated urban areas such as Beijing, Dhaka, Kanpur, and Hanoi, but was seen generally across many SPARTAN sites.

The enrichment of potentially harmful elements in fine particulate matter from anthropogenic sources is of global relevance to public health and warrants further attention. For example, we found in Dhaka and Kanpur that Pb concentrations exceeded the US National Ambient Air Quality 3-month guideline of 150 ng/m^3 , and that concentrations of the carcinogen As approached or exceeded the World Health Organization's 1:100,000 excess lifetime risk level (6.6 ng/m^3) in Kanpur, Hanoi, Beijing, and Dhaka. Emerging evidence indicates that anthropogenic fugitive, combustion, and industrial dust can comprise a significant fraction of $PM_{2.5}$ in densely populated regions⁶⁴. More generally, the high concentrations of several potentially harmful elements (e.g. Zn, Pb, Cd, Se, and As) at densely populated cities such as Beijing, Dhaka, Kanpur, and Hanoi motivate expanded measurements in other cities worldwide, especially in rapidly developing economies.

Materials and methods

SPARTAN site-selection favors densely populated, globally dispersed regions that are underrepresented in terms of availability of representative and long-term air quality data. Local site-selection favors representative environments that avoid anomalous sources; low rooftops in urban environments are desirable to increase fetch, diminish local traffic influence, and offer instrument security. Locations of SPARTAN sites are shown in Fig. 6 and further site information (e.g. elevation, latitude, longitude, sampling period) is detailed in Table 2.

As SPARTAN site selection prioritizes under-sampled locations, some regions that are well-represented in terms of air quality data have not established a SPARTAN site to date. Further expansion of the network is planned for the future, in order to cover regions not sampled by SPARTAN, as well as add more sites in under-represented continents.

Sampling through SPARTAN has also occurred at several North American sites through various projects. Three pilot sites in the United States sampled in 2014–2016, and five sites located across Canada sampled over 2017–2019 as part of the MAPLE project⁶⁷. Overall filter sampling occurred over an average of 20 months across sites (range of 2 to 50 months). Over 800 $PM_{2.5}$ filters have been analyzed as of October 2019 and were included in the data set used for this study. While some sites may have lower numbers of samples, the SPARTAN sampling protocol (detailed below) was designed to better capture long-term averages in sampled PM, so even relatively few samples could be representative for the season in which they were sampled (detailed in Table 2). Ongoing measurements are expected to increase seasonal representativeness over time.

An overview of SPARTAN is provided by Snider et al.^{37,68}, in which the basis of the sampling procedure, filter analysis, and measurement ranges are presented. As the SPARTAN project developed, some aspects of the process were updated. To briefly summarize the original procedure, PM_{10} (coarse PM) and $PM_{2.5}$ filter masses were collected on a two-stage stacked filter unit inside rooftop-mounted AirPhoton SS4i automated air samplers over 9-day periods. A removable filter cartridge protected seven sequentially active pairs of coarse Nuclepore

City	Host Institute	Latitude	Longitude	Elevation (m)	Site type	Population density (/km ²) ^a	Filters sampled	First sample end date	Last sample end date	Seasons sampled in ^b
Dhaka	University of Dhaka	23.728	90.398	34	Megacity ^c	80,790	49	25-Oct-13	12-Oct-15	1,2,3,4
Bandung	Institute of Technology Bandung	- 6.888	107.610	826	Urban back-ground	22,280	78	19-Jan-14	23-Dec-16	1,2,3,4
Hanoi	Vietnam Academy of Science	21.048	105.800	40	Urban back-ground	21,430	12	09-Jun-15	09-Dec-17	1,3,4
Beijing	Tsinghua University	40.004	116.326	92	Megacity	18,300	171	03-Sep-13	05-Oct-17	1,2,3,4
Manila	Manila Observatory	14.635	121.078	63	Megacity	17,640	10	02-May-14	22-Oct-15	2,3,4
Pretoria	CSIR	- 25.757	28.280	1449	Urban back-ground	13,400	4	27-Oct-15	29-May-16	2,4
Buenos Aires	CITEDEF	- 34.555	- 58.506	26	Megacity	9160	43	11-Oct-14	14-Oct-16	1,2,3,4
Singapore	National University of Singapore	1.298	103.780	30	Urban back-ground	5460	41	14-Apr-16	14-Dec-17	1,2,3,4
Halifax	Dalhousie University	44.638	- 63.594	65	Urban back-ground	5040	56	27-Aug-17	01-Apr-19	1,2,3,4
Toronto	Environment Canada	43.790	- 79.470	186	Urban back-ground	3800	61	13-Jul-17	10-Mar-19	1,2,3,4
Kanpur	IIT Kanpur	26.513	80.232	123	Urban back-ground	3250	21	23-Dec-13	26-Sep-14	1,2,3,4
Ilorin	University of Ilorin	8.484	4.675	400	Urban back-ground	1620	17	29-Jun-14	23-Apr-19	1,2,3,4
Rehovot	Weizmann Institute	31.907	34.811	73	Urban back-ground	1440	76	22-Feb-15	03-Oct-18	1,2,3,4
Sherbrooke	Université de Sherbrooke	45.380	- 71.931	251	Urban back-ground	1190	52	06-Jul-17	20-Mar-19	1,2,3,4
Lethbridge	University of Lethbridge	49.682	- 112.869	904	Urban back-ground	590	30	03-Sep-17	23-Jan-19	1,3,4
Atlanta	Emory University	33.688	- 84.290	250	Suburban	540	21	27-Jan-14	22-Apr-14	1,2
Kelowna	Environment Canada	49.941	- 119.400	456	Suburban	61	17	10-Nov-17	06-Mar-19	1,2,4
Mammoth Cave	Mammoth Cave National Park	37.132	- 86.148	235	Natural	13	21	09-Jun-14	12-Aug-14	3
Bondville	University of Illinois	40.053	- 88.372	200	Rural	2	21	20-Aug-15	14-Apr-16	1,2,3,4

Table 2. SPARTAN site-by-site information. Sites are sorted from highest population density to lowest. ^aPopulation density is reported for a 1 km radius based on NASA's Gridded Population of the World⁶⁵. ^bFor concision, seasons are labelled as such: 1—Dec–Feb, 2—Mar–May, 3—Jun–Aug, 4—Sept–Nov. ^cMegacities are defined as having 10 million or more inhabitants⁶⁶.

and fine Teflon filters, plus a pair of travelling blanks. Beginning in late 2017, sampling stations at SPARTAN were upgraded to the AirPhoton SS5 models, which use a cyclone inlet to separate particles by varying flow rates through the station (5 and 1.5 L/min, respectively, for PM_{2.5} and PM₁₀ size-cuts). This allowed for elimination of the Nuclepore filters and the introduction of filter cartridges with eight total stretched Teflon filters that included six sampling PM_{2.5}, one sampling PM₁₀, and one travelling blank. These cartridges were pre-assembled in the SPARTAN central laboratories at Dalhousie University, and shipped to sites for installation by site operators.

Once the filter cartridges are installed, the sampling stations run autonomously for the cartridge duration. For international sites, each of the PM_{2.5} filters is sampled for rotating 3-h spans over 9 days, totaling 24 h of sampling. Measuring across the entire diurnal cycle over a 9-day period, rather than sampling for a consecutive 24-h period every 9 days, helps to better capture long-term averages³⁷. The PM₁₀ filter was sampled for a 30-min period after each 3-h PM_{2.5} sample for the entire 54-day sampling period, providing a 54-day average PM₁₀ concentration over a total of 24 h. For sites that are part of the MAPLE project, each filter was sampled for a total of 48 h (6-h periods for the PM_{2.5} filters and 1-h periods for the PM₁₀ filters) to ensure a quantifiable amount was deposited in these low-PM environments. Once sampling was complete, filter cartridges were removed from the sampling station, sealed, and returned to the central laboratory at Dalhousie University for chemical and physical analysis of the filters. Filters were analyzed to determine PM_{2.5} or PM₁₀ mass (gravimetric), water-soluble ions (ion chromatography with conductivity detection), black carbon (absorbance, determined through smoke-stain refractometry), and trace metals (inductively-coupled plasma mass spectrometry).

The focus of this study is trace metal content, quantified here via inductively coupled plasma mass spectrometry (ICP-MS, Thermo Scientific X-Series 2). For each filter a small quantity of isopropyl alcohol (previously 30

μL , currently $10 \mu\text{L}$) was added, then the filter was extracted (97°C for 2 h) with 5% trace metal grade nitric acid solution in a process similar to Fang et al.²⁰ and Herner et al.⁶⁹. Filters were boiled in the acidic solution and the liquid extract submitted for quantitative analysis via ICP-MS, using 25–500 ppb ($\mu\text{g/L}$) trace metals standards and three reference elements for atomic mass (^{45}Sc , ^{115}In , and ^{159}Tb) for each analysis. Measured concentrations from the field blank filters for each filter cartridge were subtracted from the seven corresponding samples of each cartridge to account for variable trace metal baselines. Consistent ICP-MS analysis in the central Dalhousie laboratory facilitated consistency of results across sites. It is established that nitric acid extraction efficiencies for some crustal elements such as Fe can be as low as 50%⁷⁰ as confirmed by our internal tests, and as such, measurement methods are being re-evaluated for future SPARTAN use. More recent analyses include the use of HCl to improve extraction efficiencies. In addition, filters will also be analyzed with XRF at Washington University. For now, this initial analysis offers perspective on this emerging dataset, with observed variability that far exceeds the factor of 2 uncertainty associated with some extraction efficiencies.

In order to compare SPARTAN trace metal measurements with independent concurrent measurements, a joint sampling campaign was conducted in the US in concert with the IMPROVE (Interagency Monitoring of Protected Visual Environments) network that has been previously described⁶⁸ and is summarized in the supplemental information (section S2).

Whole system uncertainties for the SPARTAN network are estimated through use of collocated filter sampling stations. The process is described in previous work³⁹ but briefly, three sites in typically low (Halifax, Canada), moderate (Toronto, Canada), and high (Beijing, China) PM environments performed collocated sampling over 3 week periods. Over this period, each station recorded 24-h samples (48-h in Halifax to ensure adequate loading) which were then analyzed to evaluate uncertainties across the network as further described in the supplemental material (section S3).

Received: 5 June 2020; Accepted: 27 November 2020

Published online: 11 December 2020

References

1. Brauer, M. et al. Ambient air pollution exposure estimation for the Global Burden of Disease 2013. *Environ. Sci. Technol.* <https://doi.org/10.1021/acs.est.5b03709> (2015).
2. van Donkelaar, A. et al. Global estimates of fine particulate matter using a combined geophysical-statistical method with information from satellites, models, and monitors. *Environ. Sci. Technol.* **50**, 3762–3772 (2016).
3. Cohen, A. J. et al. Estimates and 25-year trends of the global burden of disease attributable to ambient air pollution: An analysis of data from the Global Burden of Diseases Study 2015. *Lancet* [https://doi.org/10.1016/S0140-6736\(17\)30505-6](https://doi.org/10.1016/S0140-6736(17)30505-6) (2017).
4. Stanaway, J. D. et al. Global, regional, and national comparative risk assessment of 84 behavioural, environmental and occupational, and metabolic risks or clusters of risks for 195 countries and territories, 1990–2017: A systematic analysis for the Global Burden of Disease Study 2017. *Lancet* **392**, 1923–1994. [https://doi.org/10.1016/S0140-6736\(18\)32225-6](https://doi.org/10.1016/S0140-6736(18)32225-6) (2018).
5. Martin, R. V. et al. No one knows which city has the highest concentration of fine particulate matter. *Atmos. Environ. X* **3**, 100040 (2019).
6. Sun, G. et al. Oxidative interactions of synthetic lung epithelial lining fluid with metal-containing particulate matter. *Am. J. Physiol. Lung Cell Mol. Physiol.* **281**, L807–L815 (2001).
7. Wojas, B. & Almquist, C. Mass concentrations and metals speciation of $\text{PM}_{2.5}$, PM_{10} , and total suspended solids in Oxford, Ohio and comparison with those from metropolitan sites in the Greater Cincinnati region. *Atmos. Environ.* **41**, 9064–9078 (2007).
8. Boohene, M., Sulemana, R. & Sossou, K. Assessment of Heavy Metal Concentrations in Particulate Matter (PM_{10}) in the Ambient Air of Selected Roadsides in the Accra Metropolis of Ghana, West Africa. Vol 6, 34–54 (2019).
9. Hama, S. M. L., Cordell, R. L., Staelens, J., Mooibroek, D. & Monks, P. S. Chemical composition and source identification of PM_{10} in five North Western European cities. *Atmos. Res.* **214**, 135–149 (2018).
10. Negral, L. et al. Anthropogenic and meteorological influences on PM_{10} metal/semi-metal concentrations: Implications for human health. *Chemosphere* **243**, 125347 (2020).
11. Maione, M. et al. Air quality and climate change: Designing new win-win policies for Europe. *Environ. Sci. Policy* **65**, 48–57 (2016).
12. Øvrevik, J., Refsnes, M., Låg, M., Holme, J. A. & Schwarze, P. E. Activation of proinflammatory responses in cells of the airway mucosa by particulate matter: Oxidant- and non-oxidant-mediated triggering mechanisms. *Biomolecules* **5**, 1399–1440 (2015).
13. West, J. J. et al. What we breathe impacts our health: Improving understanding of the link between air pollution and health. *Environ. Sci. Technol.* **50**, 4895–4904 (2016).
14. Lippmann, M. Toxicological and epidemiological studies of cardiovascular effects of ambient air fine particulate matter ($\text{PM}_{2.5}$) and its chemical components: Coherence and public health implications. *Crit. Rev. Toxicol.* **44**, 299–347 (2014).
15. Gent, J. F. et al. Symptoms and medication use in children with asthma and traffic-related sources of fine particle pollution. *Environ. Health Perspect.* **117**, 1168–1174 (2009).
16. Kampa, M. & Castanas, E. Human health effects of air pollution. *Environ. Pollut.* **151**, 362–367 (2008).
17. Rajagopalan, S. & Brook, R. D. Air pollution and type 2 diabetes: Mechanistic insights. *Diabetes* **61**, 3037–3045 (2012).
18. Chirizzi, D. et al. Influence of Saharan dust outbreaks and carbon content on oxidative potential of water-soluble fractions of $\text{PM}_{2.5}$ and PM_{10} . *Atmos. Environ.* **163**, 1–8 (2017).
19. Pardo, M., Shafer, M. M., Rudich, A., Schauer, J. J. & Rudich, Y. Single exposure to near roadway particulate matter leads to confined inflammatory and defense responses: Possible role of metals. *Environ. Sci. Technol.* <https://doi.org/10.1021/acs.est.5b01449> (2015).
20. Fang, T., Guo, H., Verma, V., Peltier, R. E. & Weber, R. J. $\text{PM}_{2.5}$ water-soluble elements in the southeastern United States: Automated analytical method development, spatiotemporal distributions, source apportionment, and implications for health studies. *Atmos. Chem. Phys.* **15**, 11667–11682 (2015).
21. Weichenthal, S. et al. Spatial variations in the estimated production of reactive oxygen species in the epithelial lung lining fluid by iron and copper in fine particulate air pollution. *Environ. Epidemiol.* **2**, e020 (2018).
22. Weichenthal, S. et al. Oxidative burden of fine particulate air pollution and risk of cause-specific mortality in the Canadian Census Health and Environment Cohort (CanCHEC). *Environ. Res.* **146**, 92–99 (2016).
23. Gottipolu, R. R. et al. Cardiopulmonary responses of intratracheally instilled tire particles and constituent metal components. *Inhalation. Toxicol.* **20**, 473–484 (2008).
24. Li, Q. et al. The preferential accumulation of heavy metals in different tissues following frequent respiratory exposure to $\text{PM}_{2.5}$ in rats. *Sci. Rep.* **5**, 16936 (2015).

25. IARC. *Air Pollution and Cancer*, IARC publication no. 161. (2013).
26. Bellinger, D., Leviton, A., Waternaux, C., Needleman, H. & Rabinowitz, M. Longitudinal analyses of prenatal and postnatal lead exposure and early cognitive development. *N. Engl. J. Med.* **316**, 1037–1043 (1987).
27. Gibson, M. D. *et al.* A comparison of four receptor models used to quantify the boreal wildfire smoke contribution to surface PM_{2.5} in Halifax, Nova Scotia during the BORTAS-B experiment. *Atmos. Chem. Phys.* **15**, 815–827 (2015).
28. Cohen, D. D., Stelcer, E., Hawas, O. & Garton, D. IBA methods for characterisation of fine particulate atmospheric pollution: A local, regional and global research problem. *Nucl. Instrum. Methods Phys. Res. Sect. B Beam Interact. Mater. Atoms.* **219–220**, 145–152 (2004).
29. Betha, R., Behera, S. N. & Balasubramanian, R. 2013 Southeast Asian smoke haze: Fractionation of particulate-bound elements and associated health risk. *Environ. Sci. Technol.* **48**, 4327–4335 (2014).
30. Councill, T. B., Duckenfield, K. U., Landa, E. R. & Callender, E. Tire-wear particles as a source of zinc to the environment. *Environ. Sci. Technol.* **38**, 4206–4214 (2004).
31. Pacyna, J. M. & Pacyna, E. G. An assessment of global and regional emissions of trace metals to the atmosphere from anthropogenic sources worldwide. *Environ. Rev.* **9**, 269–298 (2001).
32. Gibson, M. D. *et al.* Identifying the sources driving observed PM_{2.5} temporal variability over Halifax, Nova Scotia, during BORTAS-B. *Atmos. Chem. Phys.* **13**, 7199–7213 (2013).
33. Wang, X., Bi, X., Sheng, G. & Fu, J. Chemical composition and sources of PM₁₀ and PM_{2.5} aerosols in Guangzhou. *China Environ. Monit. Assess.* **119**, 425–439 (2006).
34. Grigoratos, T. & Martini, G. Brake wear particle emissions: A review. *Environ. Sci. Pollut. Res.* **22**, 2491–2504 (2015).
35. Wai, K.-M., Wu, S., Li, X., Jaffe, D. A. & Perry, K. D. Global atmospheric transport and source-receptor relationships for arsenic. *Environ. Sci. Technol.* **50**, 3714–3720 (2016).
36. Rauch, J. N. & Pacyna, J. M. Earth's global Ag, Al, Cr, Cu, Fe, Ni, Pb, and Zn cycles. *Glob. Biogeochem. Cycles* **23**, GB2001 (2009).
37. Snider, G. *et al.* SPARTAN: A global network to evaluate and enhance satellite-based estimates of ground-level particulate matter for global health applications. *Atmos. Meas. Tech.* **8**, 505–521 (2015).
38. Park, R. J., Jacob, D. J., Chin, M. & Martin, R. V. Sources of carbonaceous aerosols over the United States and implications for natural visibility. *J. Geophys. Res. Atmos.* <https://doi.org/10.1029/2002jd003190> (2003).
39. Weagle, C. L. *et al.* Global sources of fine particulate matter: Interpretation of PM_{2.5} chemical composition observed by SPARTAN using a global chemical transport model. *Environ. Sci. Technol.* **52**, 11670–11681 (2018).
40. Taylor, S. R. & McLennan, S. M. The geochemical evolution of the continental crust. *Rev. Geophys.* **33**, 241–265 (1995).
41. Hsu, S. C. *et al.* High wintertime particulate matter pollution over an offshore island (Kinmen) off southeastern China: An overview. *J. Geophys. Res. Atmos.* **115**, D17309 (2010).
42. Cesari, D. *et al.* Analysis of raw soils and their re-suspended PM₁₀ fractions: Characterisation of source profiles and enrichment factors. *Appl. Geochem.* **27**, 1238–1246 (2012).
43. Malm, W. C., Sisler, J. F., Huffman, D., Eldred, R. A. & Cahill, T. A. Spatial and seasonal trends in particle concentration and optical extinction in the United States. *J. Geophys. Res.* **99**, 1347–1370 (1994).
44. Malm, W. C. & Hand, J. L. An examination of the physical and optical properties of aerosols collected in the IMPROVE program. *Atmos. Environ.* **41**, 3407–3427 (2007).
45. Behera, S. N. & Sharma, M. Reconstructing primary and secondary components of PM_{2.5} composition for an urban atmosphere. *Aerosol Sci. Technol.* **44**, 983–992 (2010).
46. Zhang, J., Wu, Y., Liu, C. L., Shen, Z. B. & Zhang, Y. Major components of aerosols in North China: Desert region and the yellow sea in the spring and summer of 1995 and 1996. *J. Atmos. Sci.* **59**, 1515–1532 (2002).
47. Das, R. *et al.* Trace element composition of PM_{2.5} and PM₁₀ from Kolkata—a heavily polluted Indian metropolis. *Atmos. Pollut. Res.* **6**, 742–750 (2015).
48. EPA. National Ambient Air Quality Standards (NAAQS). NAAQS 1 (2014).
49. Salam, A., Bauer, H., Kassim, K., Ullah, S. M. & Puxbaum, H. Aerosol chemical characteristics of a mega-city in Southeast Asia (Dhaka-Bangladesh). *Atmos. Environ.* **37**, 2517–2528 (2003).
50. Islam, M. F. *et al.* Trace metals concentrations at the atmosphere particulate matters in the Southeast Asian Mega City (Dhaka, Bangladesh). *Open J. Air Pollut.* **04**, 86–98 (2015).
51. WHO, W. H. O. Air quality guidelines for Europe. (2000).
52. Garcia-Aleix, J. R., Delgado-Saborit, J. M., Verdú-Martin, G., Amigó-Descarrega, J. M. & Esteve-Cano, V. Trends in arsenic levels in PM₁₀ and PM_{2.5} aerosol fractions in an industrialized area. *Environ. Sci. Pollut. Res.* **21**, 695–703 (2013).
53. Okuda, T. *et al.* Daily concentrations of trace metals in aerosols in Beijing, China, determined by using inductively coupled plasma mass spectrometry equipped with laser ablation analysis, and source identification of aerosols. *Sci. Total Environ.* **330**, 145–158 (2004).
54. Pacyna, E. G. *et al.* Current and future emissions of selected heavy metals to the atmosphere from anthropogenic sources in Europe. *Atmos. Environ.* **41**, 8557–8566 (2007).
55. Liu, G. J. *et al.* Health effects of arsenic, fluorine, and selenium from indoor burning of Chinese coal. *Rev. Environ. Contam. Toxicol.* **189**, 89–106 (2007).
56. Duan, J. & Tan, J. Atmospheric heavy metals and Arsenic in China: Situation, sources and control policies. *Atmos. Environ.* **74**, 93–101 (2013).
57. Santoso, M. *et al.* Long term airborne lead pollution monitoring in Bandung, Indonesia. *Int. J. PIXE* **24**, 151–159 (2014).
58. Zakiyya, H., Distya, Y. D. & Ellen, R. A review of spent lead-acid battery recycling technology in Indonesia: comparison and recommendation of environment-friendly process. In *IOP Conference Series: Materials Science and Engineering* Vol. 288, (Institute of Physics Publishing, 2018).
59. Habibu, S. *et al.* A review on industrial effluents as major sources of water pollution in Nigeria riverbank filtration and surface water pollution view project electrochemical sensor view project a review on industrial effluents as major sources of water pollution in Nigeria. *Chem. J.* **1**, 159–164 (2015).
60. Balasubramanian, R. & Qian, W. B. Characterization and source identification of airborne trace metals in Singapore. *J. Environ. Monit.* **6**, 813–818 (2004).
61. EMA. *Singapore Energy Statistics*. (2017).
62. Querol, X. *et al.* Speciation and origin of PM₁₀ and PM_{2.5} in selected European cities. *Atmos. Environ.* **38**, 6547–6555 (2004).
63. Amato, F., Alastuey, A., Karanasiou, A. & Lucarelli, F. AIRUSE-LIFE+: A harmonized PM speciation and source apportionment in 5 Southern European cities. *Artic. Atmos. Chem. Phys.* <https://doi.org/10.5194/acpd-15-23989-2015> (2015).
64. Philip, S. *et al.* Anthropogenic fugitive, combustion and industrial dust is a significant, underrepresented fine particulate matter source in global atmospheric models. *Environ. Res. Lett.* **12**, 044018 (2017).
65. University, C. for I. E. S. I. N.-C.-C. Gridded Population of the World, Version 4 (GPWv4): Population Count. (2016).
66. World Urbanization Prospects—Population Division—United Nations. <https://population.un.org/wup/Publications/>. Accessed 9 Dec 2019.
67. Brauer, M. *et al.* MAPLE: Mortality-air pollution associations in low exposure environments. In *2019 HEI Conference*, (2019).
68. Snider, G. *et al.* Variation in global chemical composition of PM_{2.5}: Emerging results from SPARTAN. *Atmos. Chem. Phys.* **16**, 9629–9653 (2016).

69. Herner, J. D., Green, P. G. & Kleeman, M. J. Measuring the trace elemental composition of size-resolved airborne particles. *Environ. Sci. Technol.* **40**, 1925–1933 (2006).
70. Roje, V. Multi-elemental analysis of marine sediment reference material MESS-3: One-step microwave digestion and determination by high resolution inductively coupled plasma-mass spectrometry (HR-ICP-MS). *Chem. Pap.* **64**, 409–414 (2010).

Acknowledgements

This work was supported by Bloomberg Philanthropies through the Health Effects Institute, by the Climate-Works Foundation, and by the Natural Sciences and Engineering Research Council (NSERC) of Canada. We thank the HERC labs for supplying filter weighing facilities. Data collection in Kanpur was supported by grant from the Indo-US Science and Technology Forum (IUSSTF) under real time air quality monitoring scheme. Data collection in Rehovot was supported in part by the Environmental Health Fund (Israel) and the Israel Science Foundation (grant #236/16). Partial support for the ITB site was by Ministry of Research, Technology & Higher Education, under World Class University (WCU) managed by Bandung Institute of Technology (ITB). The views expressed here are of authors and do not necessarily reflect those of NAS or USAID. The Singapore site was supported by the Singapore National Research Foundation (NRF) through the Singapore-MIT Alliance for Research and Technology (SMART), Center for Environmental Sensing and Modeling. The site in Atlanta was partially supported by NASA Applied Science Program (Grant # 80NSSC19K0191) and the Jet Propulsion Laboratory (Contract #1588347 and #1363692). All data are freely available as a public good at <http://www.spartan-network.org>. We welcome expression of interest to collaborate with this grass-roots network.

Author contributions

All listed authors of this work have contributed substantially to this research in some capacity, and have approved this manuscript. Contributions were as such: core SPARTAN team (data collection, data analysis, experimental design, drafting of manuscript): J.M., G.S., C.L.W., B.W., P.B., E.S., R.V.M., M.B., Y.R. SPARTAN site principal investigators and site operators (data collection): I.A., C.A., N.X.A., R.B., C.C., J.D., R.M.G., K.H., N.L., P.L., Y.L., F.J., K.S.J., A.M., L.K.N., E.J.Q., A.S., S.N.T., Q.Z. SPARTAN network partners (experimental design): J.R.B., A.C., B.N.H., R.K., J.V.M., B.S., C.W. Laboratory research partners (data collection and analysis): G.G., J.S.K., M.D.G.

Competing interests

The authors declare no competing interests.

Additional information

Supplementary Information The online version contains supplementary material available at <https://doi.org/10.1038/s41598-020-78789-y>.

Correspondence and requests for materials should be addressed to R.V.M.

Reprints and permissions information is available at www.nature.com/reprints.

Publisher's note Springer Nature remains neutral with regard to jurisdictional claims in published maps and institutional affiliations.



Open Access This article is licensed under a Creative Commons Attribution 4.0 International License, which permits use, sharing, adaptation, distribution and reproduction in any medium or format, as long as you give appropriate credit to the original author(s) and the source, provide a link to the Creative Commons licence, and indicate if changes were made. The images or other third party material in this article are included in the article's Creative Commons licence, unless indicated otherwise in a credit line to the material. If material is not included in the article's Creative Commons licence and your intended use is not permitted by statutory regulation or exceeds the permitted use, you will need to obtain permission directly from the copyright holder. To view a copy of this licence, visit <http://creativecommons.org/licenses/by/4.0/>.

© The Author(s) 2020